Structure and Bonding of a Site-Isolated Transition Metal Complex: Rhodium Dicarbonyl in Highly Dealuminated Zeolite Y

Jesse F. Goellner,[†] Bruce C. Gates,*[,†] Georgi N. Vayssilov,[‡,§] and Notker Rösch*[,‡]

Contribution from the Department of Chemical Engineering and Materials Science, University of California, Davis, California 95616, and Institut für Physikalische und Theoretische Chemie, Technische Universität München, 85747 Garching, Germany

Received April 6, 2000

Abstract: The structure and bonding of rhodium dicarbonyl bonded to highly dealuminated zeolite Y has been determined by the combined application of extended X-ray absorption fine structure (EXAFS) and infrared spectroscopies and quantum chemical calculations based on density functional theory. The EXAFS and infrared spectra indicate the existence of nearly unique rhodium dicarbonyl species bonded at structurally equivalent positions in the zeolite pores. However, even this anchored structure, one of the simplest known, is not determined fully by the experimental results, and quantum chemical calculations were needed to eliminate the ambiguity. Taken together, the experimental and theoretical results indicate $Rh^+(CO)_2$ located at a four-ring of the faujasite framework; the rhodium center is bonded to two oxygen centers of the framework near an aluminum center with a Rh−O distance of 2.15−2.20 Å. The results show how spectroscopy and theory used in combination can determine the structure and location of a metal complex anchored to a structurally uniform support.

Introduction

Mononuclear metal complexes supported on solid surfaces are important technological catalysts, e.g., for alkene polymerization.[1−4] Determination of the structure and location of a supported metal complex, including the metal−support bonding, is challenging because the structures are typically nonuniform. Structure determination is in prospect most easily accomplished when the supported metal complex is a simple molecular analogue, which requires that the support be uniform (crystalline) in structure, so that bonding of the complex takes place at equivalent surface sites; a full structure determination requires a characterization of the metal−support bonds. Here we report the characterization of rhodium dicarbonyl in a zeolite. We chose this sample because metal carbonyls are among the simplest and most widely investigated supported metal complexes and zeolites are crystalline and therefore offer a relatively uniform set of surface sites for bonding a metal complex.

Metal carbonyls on amorphous metal oxides typically have broad CO peaks in the infrared spectra indicative of nonuniform surfaces with multiple bonding surface sites for the complex. Metal carbonyls bonded to zeolites are characterized by somewhat narrower infrared bands than the corresponding complexes on amorphous metal oxides, as illustrated by the spectra of $Rh^+(CO)_2$ in the faujasite zeolite NaY.[5] The work of Miessner et al.[6] shows that even sharper bands (with full width at half-maximum of less than 5 cm^{-1}) characterize metal carbonyls in dealuminated zeolite Y (DAY). These spectra imply nearly uniform sites for the bonding of $Rh^+(CO)_2$. Thus, samples such as these offer excellent opportunities for deeper understanding of structures of supported metal complexes and metal−support bonding.

Miessner et al.[6] provided only indirect evidence (from analysis of bands in the hydroxyl stretching region of the infrared spectrum) of how the metal complex bonds to the support. Thus, we were motivated to characterize the structure by extended X-ray absorption fine structure (EXAFS) spectroscopy. Because the samples reported earlier[6] were prepared from aqueous solutions of $[Rh(NH_3)_5Cl][OH]_2$, we infer that EXAFS data characterizing them could be complicated by Rh−Cl contributions. Consequently, we used a chloride-free precursor instead, dicarbonylacetylacetonato rhodium(I), $[Rh(CO)_2(acac)]$, with ligands that could be removed from the support during the formation of the supported rhodium carbonyl. Even with this simplification, however, we recognize that metal-edge EXAFS data are often less than sufficient for unambiguous determination of metal−support bonding,[7,8] and thus a complementary goal was to use theory to discriminate between models developed from the spectroscopic data. The results show that the application of EXAFS and infrared spectroscopies combined with quantum chemical computations (based on density functional theory, DFT) offers the opportunity for incisive structural characterization of uniform supported metal complexes, including a representation of the transition metal and the ligands as well as the support.[9,10]

* To whom correspondence should be addressed.
[†] University of California.
[‡] Technische Universität München.
[§] Permanent address: Faculty of Chemistry, University of Sofia, 1126 Sofia, Bulgaria. E-mail: gnv@chem.uni-sofia.bg.

(1) Kristen, M. O. *Top. Catal.* **1999**, *7*, 89.
(2) Kaminsky, W. *Sci. Technol. Catal. 1998* **1999**, *121*, 3.
(3) Kaminsky, W. *Angew. Makromol. Chem.* **1994**, *223*, 101.
(4) Roscoe, S. B.; Frechet, J. M. J.; Walzer, J. F.; Dias, A. J. *Science* **1998**, *280*, 270.
(5) Weber, W. A. Ph.D. Dissertation, University of California, Davis, 1998.
(6) Miessner, H.; Burkhardt, I.; Gutschick, D.; Zecchina, A.; Morterra, C.; Spoto, G. *J. Chem. Soc., Faraday Trans. 1* **1989**, *85*, 2113.
(7) Binsted, N.; Evans, J.; Greaves, G. N.; Price, R. J. *Organometallics* **1989**, *8*, 613.
(8) van't Blik, H. F. J.; van Zon, J. B. A. D.; Huzinga, T.; Vis, J. C.; Koningsberger, D. C.; Prins, R. *J. Am. Chem. Soc.* **1985**, *107*, 3139.

10.1021/ja001209f CCC: $19.00
Published on Web 08/06/2000

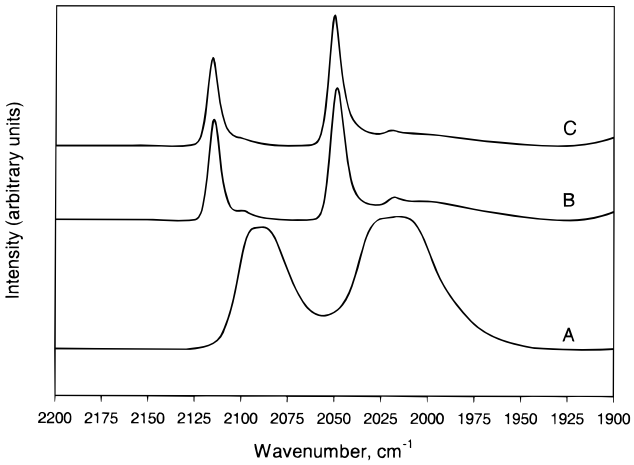

Figure 1. Infrared spectra in the carbonyl stretching region of Y zeolite-supported $Rh^+(CO)_2$: (A) NaY zeolite calcined at 200 °C; (B) dealuminated Y zeolite calcined at 120 °C; and (C) dealuminated Y zeolite calcined at 300 °C.

Results

Spectroscopic Evidence of Zeolite-Supported Rhodium Dicarbonyl. (a) Spectral Evidence of Site-Isolated Surface Complex. In the following we discuss evidence that each sample contains predominately site-isolated rhodium dicarbonyl bonded to highly dealuminated zeolite Y. The infrared peaks of $Rh^+(CO)_2$ in DAY calcined at either 300 or 120 °C are extremely narrow and have an excellent signal-to-noise ratio (Figure 1). The fact that these peaks are so narrow eliminates the possibility of multilayers of $[Rh(CO)_2(acac)]$ on the support. Uniformity of the surface species and the bonding of $Rh^+(CO)_2$ to the zeolite are indicated qualitatively by the straightforward identification of spectral contributions (coordination shells) in the EXAFS spectra without accompanying high noise level or distortion and broadening of the peaks. The Rh−CO contributions determined by EXAFS spectroscopy, Rh−C and Rh−O* (O* is carbonyl oxygen), are consistent with the presence of rhodium dicarbonyl groups in each sample. No Rh−Rh contributions are present in the EXAFS data, indicating that the samples do not consist of carbonyls terminally bonded to rhodium crystallites or $[Rh(CO)_2(acac)]$ multilayers. The high quality of the infrared and EXAFS spectra implies a unique position for $Rh^+(CO)_2$ in the zeolite. Consequently, these samples offer one of the best opportunities yet recognized for determining the precise bonding site for a metal complex isolated on a support and might be regarded as prototypical.

(b) Infrared Spectra. The positions of the ν_{CO} vibrational bands representing $Rh^+(CO)_2$ on DAY calcined at either 300 or 120 °C are the same (within the experimental resolution) as those reported by Miessner et al.[6] for DAY-supported $Rh^+(CO)_2$ formed by incipient wetness impregnation of the zeolite with $[Rh(NH_3)_5Cl][OH]_2$ followed by calcination at 400 °C and subsequent oxidative fragmentation[11] by CO (Table 1). Our ν_{CO} peaks (Figure 1) are narrow, in agreement with Miessner's results.[6] From the ratio of the intensities of the symmetric and anti-symmetric C−O stretching peaks,[12] the C−Rh−C bond angle of the supported $Rh^+(CO)_2$ was calculated to be approximately 101 and 98° for the samples calcined at 300 and 120 °C, respectively. Miessner et al.[6] reported a value of 106°.

The spectra show that our samples calcined at 120 and at 300 °C are nearly identical with each other and to those of Miessner. From the splitting of the C−O stretching band into a doublet and the shift of the satellite bands with respect to the main bands, we conclude that our supported complexes were rhodium dicarbonyls.[13] The O−H stretching region of the infrared spectrum of our sample calcined at 300 °C more nearly matches that of Miessner's sample calcined at 400 °C than does the spectrum of our sample calcined at 120 °C, corresponding to the greater dehydration of the former two samples.[14]

(c) EXAFS Spectra. The EXAFS results (Tables 2 and 3 and Figures 2−5) show the plausibility of three models of the local structure of the rhodium complex, referred to as Models I, II, and III (Tables 2 and 3). Consistent with the presence of two CO ligands per Rh atom, each model includes Rh−CO contributions (Rh−C at approximately 1.9 Å and Rh−O* at approximately 3.0 Å). The models differ from each other in the nature of the Rh−support contributions. Each includes a short Rh−support oxygen contribution, $Rh-O_{short}$, at approximately 2.1 Å for Models I and III and at approximately 2.2 Å for Model II. The remaining Rh−support contributions in Models I and II are Rh−Al at approximately 2.8 Å and Rh−O at approximately 3.3 Å. The remaining Rh−support contributions in Model III are $Rh-O_{long}$ at approximately 2.8 Å and Rh−T (T = Al, Si) at approximately 3.4 Å. The longer Rh−support contributions at about 3.3−3.4 Å in each model (Rh−O in Models I and II and Rh−Al in Model III) were included to achieve satisfactory fits of the data, but these contributions are small and only tentatively assigned and would have been left out of a typical, less detailed, EXAFS analysis.

The number of parameters used in fitting each model is 20; the numbers justified statistically by the Nyquist theorem[15] are 21 and 22 for the samples calcined at 120 and at 300 °C, respectively. The fitting ranges in both momentum (k) and real (r) space (shown in Supporting Information) were determined by the data quality.

The three models all fit the data well, and the quality of the fit varies barely, if at all, from one model to the other. The value of fit diagnostic parameters, ϵ_ν^2 (goodness of fit),[15] and the variances between the data and model prediction for the EXAFS function, χ, and the Fourier transform of χ (for k^0-,

(9) Hu, A.; Neyman, K. M.; Staufer, M.; Belling, T.; Gates, B. C.; Rösch, N. *J. Am. Chem. Soc.* **1999**, *121*, 4522.

(10) Ferrari, A. M.; Neyman, K. M.; Mayer, M.; Staufer, M.; Gates, B. C.; Rösch, N. *J. Phys. Chem. B* **1999**, *103*, 5311.

(11) Lamb, H. H.; Gates, B. C.; Knözinger, H. *Angew. Chem., Int. Ed. Engl.* **1988**, *27*, 1127.

(12) Braterman, P. S. *Metal Carbonyl Spectra*; Academic Press: New York, 1975.

(13) We rule out the possibility that the acac ligand (or fragments formed from it) from the precursor compound was associated with the rhodium center, because the ν_{CO} region of our infrared spectrum is virtually identical with that of the samples made by Miessener[6] from rhodium salts that did not contain acac or related species. Although we conclude that the acac ligands were replaced by support oxygen ligands, we cannot rule out the possibility that acac ligands or fragments formed from them remained somewhere in the zeolite pores and remote from the rhodium centers. When $[Rh(CO)_2(acac)]$ is deposited on amorphous metal oxides, such as TiO_2, a weak, broad peak is observed in the infrared spectrum at approximately 1700 cm^{-1}, indicating remnants of the acac ligand. However, such an infrared band would be obscured in the spectrum of the zeolite DAY-supported samples reported here by the absorption of the zeolite.

(14) The O−H stretching regions of the infrared spectra of our samples (Figure 1 in Supporting Information) are more complicated than Miessner's.[6] A peak at 3736 cm^{-1} in the spectrum of the sample calcined at 300 °C matches Miessner's peak at 3739 cm^{-1}.[6] During the early stages of formation of supported $Rh^+(CO)_2$ from supported aggregates of rhodium metal, Miessner et al. observed peaks which correspond to acidic OH groups. Such peaks were not observed in the spectrum of our sample calcined at 300 °C. In contrast, the O−H stretching region characterizing our sample calcined at 120 °C, which had a higher concentration of surface water than that calcined at 300 °C, exhibits broad and muted OH features that do not allow clear identification of band positions (Figure 1 in Supporting Information).

(15) Lytle, F. W.; Sayers, D. E.; Stern, E. A. *Physica B* **1989**, *158*, 701.

Table 1. Summary of Infrared Spectra of Zeolite DAY-Supported $Rh^+(CO)_2$ and Calculated C−O Frequencies

sample (support calcination temp, °C)	CO freq (cm^{-1}) main doublet	CO freq (cm^{-1}) satellite bands[c]	I_{sym}/I_{asym}[a]	C−Rh−C angle (deg)[b]
experimental				
$Rh(CO)_2$(acac) in THF	2081 s, 2010 vs	2062 vw, 1980 vw	0.64	103
DAY (120)[d]	2115 s, 2049 vs	2100 vw, 2018 vw	0.75	98
DAY (300)[d]	2116 s, 2050 vs	2108 vw, 2020 vw	0.67	101
DAY (400)[e]	2118 s, 2053 vs	2108 vw, 2021 vw	0.57	106
calculated[f]				
zeolite model cluster T4[g]	2114, 2060	2100, 2025	0.72	99[h]
free $Rh^+(CO)_2$	2172, 2124	2157, 2088		

[a] Intensity ratio of symmetric and antisymmetric modes. [b] C−Rh−C angle deduced from the value of I_{sym}/I_{asym}. [c] Modes corresponding to a complex incorporating one ^{12}CO ligand and one ^{13}CO ligand. [d] Sample prepared by adsorption of $[Rh(CO)_2(acac)]$ on zeolite DAY calcined at 120 or 300 °C. [e] Rhodium-exchanged DAY zeolite calcined at 400 °C and dosed with CO.[6] [f] C−O stretching mode corrected with +32 cm^{-1} according to the difference between calculated harmonic frequency 2111 cm^{-1} and experimental frequency 2143 cm^{-1}. [g] See text and Figure 7 for a description of the model. [h] The C−Rh−C angle obtained from the geometry optimization is 90.4°.

Table 2. EXAFS Parameters[a] Characterizing Samples Made from Chemisorption of $[Rh(CO)_2(acac)]$ on Dealuminated Y Zeolite

calcination temp (°C) of the zeolite support	calcd[b]			Model I					Model II					Model III				
	dist	*N*	*R*, (Å)	back-scatterer	*N*	*R* (Å)	$10^3\Delta\sigma^2$ ($Å^2$)	ΔE_0 (eV)	back-scatterer	*N*	*R* (Å)	$10^3\Delta\sigma^2$ ($Å^2$)	ΔE_0 (eV)	back-scatterer	*N*	*R* (Å)	$10^3\Delta\sigma^2$ ($Å^2$)	ΔE_0 ((eV)
300				CO					CO					CO				
	Rh−C	2	1.88	C	2.4	1.86	0.20	−8.80	C	2.2	1.86	−0.96	−16.45	C	2.2	1.86	0.24	−13.66
	Rh−O*	2	3.03	O*	1.9	2.99	1.43	−11.27	O*	2.3	2.96	0.49	−7.47	O*	2.3	3.00	−0.16	−13.86
				support					support					support				
	Rh−O	2	2.19−2.20	O_{short}	3.1	2.09	1.26	5.17	O_{short}	1.9	2.15	0.61	−9.42	O_{short}	1.9	2.09	1.19	3.01
	Rh−Al	1	2.80	Al	1.1	2.75	0.66	−25.22	Al	1.1	2.73	0.88	−17.29	O_{long}	1.1	2.81	−4.00	−10.43
	Rh−X	1	3.24−3.33	O	0.7	3.29	−7.62	−2.57	O	1.0	3.31	−5.54	−11.98	Al	1.0	3.40	0.48	19.70
120				CO					CO					CO				
	Rh−C	2	1.88	C	2.4	1.86	−1.34	−11.28	C	2.3	1.86	−1.33	−17.17	C	2.3	1.84	0.83	−11.00
	Rh−O*	2	3.03	O*	1.9	3.05	1.87	−13.10	O*	2.2	2.97	0.69	−7.80	O*	2.2	2.99	−2.10	−8.56
				support					support					support				
	Rh−O	2	2.19−2.20	O_{short}	3.5	2.10	3.08	2.59	O_{short}	1.8	2.16	−0.32	−9.30	O_{short}	1.8	2.12	−0.62	−0.41
	Rh−Al	1	2.80	Al	1.3	2.75	0.06	−27.78	Al	1.3	2.74	0.38	−19.71	O_{long}	1.3	2.80	−7.70	−10.30
	Rh−X	1	3.24−3.33	O	0.3	3.29	−11.38	8.34		1.3	3.31	−3.82	−11.25	Al	1.3	3.39	2.91	19.81

[a] Commonly accepted error bounds on structural parameters obtained by EXAFS spectroscopy are *N*, ±10%; *R*, ±0.02 Å; $\Delta\sigma^2$, ±20%; and ΔE_0, ±20%.[17] [b] Calculated for the complex $Rh^+(CO)_2$ adsorbed at the cluster T4 using a density functional method (this work).

Table 3. Binding Energies (BE, kJ/mol) and Distances (Å) for Rh^+ Ion Located at the Model Clusters As Obtained from the Density Functional Calculations

cluster	T4	T5	T6
BE	589	577	613
distances			
Rh−O(Al)[a]	2.20, 2.25	2.22, 2.41, 2.45	2.25, 2.25
Rh−O(Si)[b]	2.68, 3.39	3.88, 4.45	2.51, 2.57, 2.71, 2.78
Rh−Al	2.93	2.64	3.06

[a] Distance to oxygen centers connected to Al. [b] Distance to oxygen centers between two Si.

k^1-, k^2-, and k^3-weighting of the data) are summarized in the Supporting Information.[16]

Within the uncertainties associated with the EXAFS data, the Rh−CO contributions are essentially the same for the two samples and the three models. Within the expected uncertainty, the Rh−C coordination numbers (2.2−2.4) do not differ from the value 2 for rhodium dicarbonyl.[17] The same holds true for the Rh−O* coordination numbers (1.8−2.3), which essentially match the expected value of 2. The Rh−C distances for each sample and each model match the distance (1.86 Å) typical of rhodium complexes with terminal CO ligands.[18] The Rh−O* distances are approximately 3.0 Å, a few hundredths of an angstrom shorter than expected for rhodium complexes of a terminally bound CO.[19]

Within the error associated with the EXAFS technique, Model I and Model III are represented by the same $Rh-O_{short}$ distance; the values are 2.09 Å for $Rh^+(CO)_2$ supported by the zeolite calcined at 300 °C and 2.10−2.12 Å for the zeolite calcined at 120 °C. Model II represents these same samples with slightly greater $Rh-O_{short}$ distances of 2.15−2.16 Å.[20]

The three models differ from each other in the coordination numbers characterizing the $Rh-O_{short}$ contribution, i.e., how many support oxygen atoms constitute the multidentate ligand bonded to the Rh atom. The values of Model I are 3.1 and 3.5 for samples calcined at 300 and at 120 °C, respectively. The

(16) The match between the calculated EXAFS-derived models and the data is slightly better for the sample calcined at 300 °C than for that calcined at 120 °C. The qualities of the fits obtained with Models I and III are essentially the same and slightly higher than that of the fit obtained with Model II. As shown in Figure 2 in the Supporting Information for $Rh^+(CO)_2$ supported in the zeolite calcined at 300 °C, the residuals for each model are of almost the same magnitude as the standard deviation of the data; consequently, the small differences in the fit diagnostics between the three models mainly reflect which model better matches the noise in the data. An F-test based on values of ϵ_ν^2 showed that the probabilities that Model III describes the data better than Model I are only 51% and 50% for samples calcined at 300 and 120 °C, respectively. Similar values, with no probability exceeding 61%, were obtained for similar comparisons discriminating between the other models. Thus, there is little basis in the data for choosing one of these models over the other, each fits the data well.

(17) Vaarkamp, M. *Catal. Today* **1998**, *39*, 271.

(18) Alexeev, O.; Gates, B. C. *Top. Catal.* **2000**, *10*, 273.

(19) The effect of multiple scattering as a consequence of the near linearity of the Rh−C−O* moiety (a shorter apparent bond distance than the actual distance) was accounted for, as well as possible, by using the Ru−O* reference described below.

(20) These are typical short metal−oxygen bonding distances for highly dispersed supported metals and supported metal complexes. For example, a $Rh-O_{short}$ contribution with a coordination number 3 and a distance of 2.12 Å was found for $Rh^+(CO)_2$ supported on γ-Al_2O_3.[8]

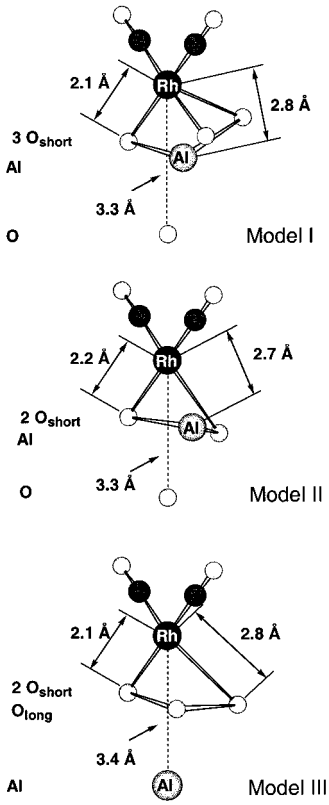

Figure 2. Simplified structural models for $Rh^+(CO)_2$ supported in dealuminated Y zeolite developed from EXAFS analysis. The figure is not meant to represent bond angles accurately as such information is not available from the EXAFS data.

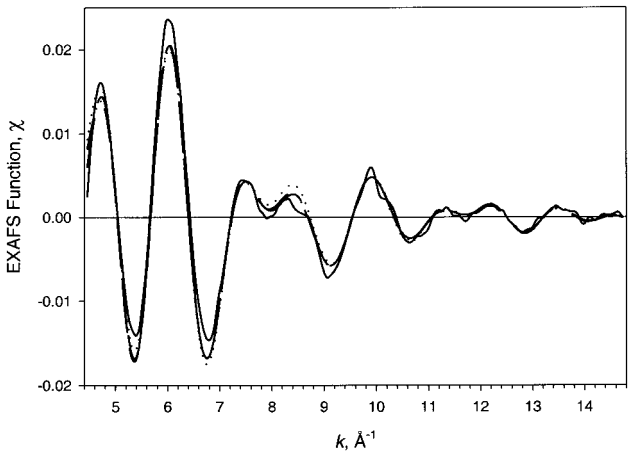

Figure 3. Results of EXAFS analysis for $Rh^+(CO)_2$ supported on dealuminated Y zeolite calcined at 300 °C: experimental EXAFS χ function (solid line) and the χ functions calculated from contributions according to Model I (dashed line), Model II (dotted line), and Model III (dashed-dotted line). The lines representing Models I and III are nearly indistinguishable for the resolution of this graph.

corresponding values are 1.9 and 1.8 for Model II and 2.4 and 2.2 for Model III. Thus, within the expected uncertainty, the EXAFS data indicate Rh−O$_{short}$ contributions with coordination numbers of 3 for Model I and 2 for Models II and III. The Debye−Waller factors characterizing the Rh−O$_{short}$ contributions differ somewhat from model to model, but the strong cross-correlation of these parameters with the Rh−O$_{short}$ coordination numbers implies a substantial uncertainty in these parameter values,[21] so that we cannot conclude that the differences are significant.

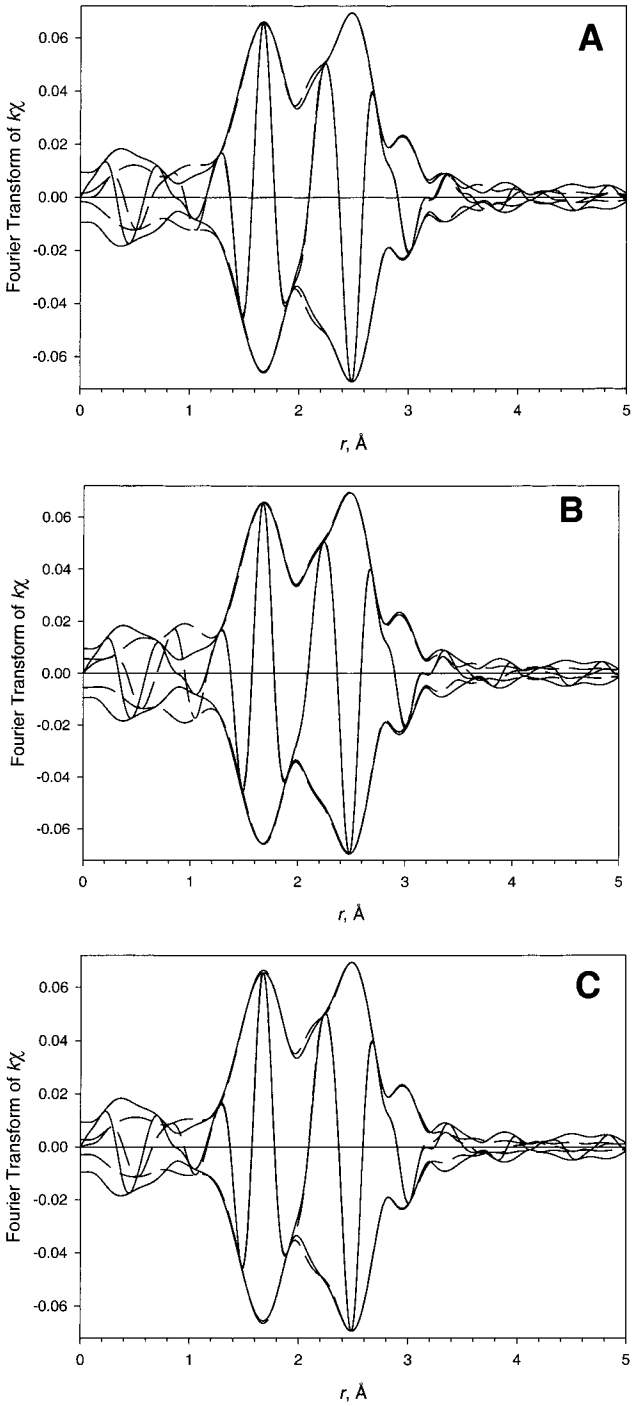

Figure 4. Results of EXAFS data analysis for $Rh^+(CO)_2$ supported on dealuminated Y zeolite calcined at 300 °C: imaginary part and magnitude of the k^1-weighted Fourier transform (Δk = 4.43−14.72 Å^{-1}) of raw data (solid lines) and calculated contributions (dashed lines) according to (A) Model I, (B) Model II, and (C) Model III.

In Model III, the remaining contributions characterizing $Rh^+(CO)_2$ supported on the zeolite calcined at 300 °C are metal−

(21) The generally accepted error bounds on structural parameters obtained by EXAFS spectroscopy are for the coordination number (N) ± 10%, the backscatterer distance (R) ± 0.02 Å, the relative Debye−Waller factor ($\Delta\sigma^2$) ± 20%, and the relative inner potential correction (ΔE_0) ± 20%.[17] However, strong cross-correlations were found between parameters of the Rh−O$_{short}$ contribution of the EXAFS spectra, regardless of which model was being evaluated. Hence, higher than typical error bars should be used when evaluating the EXAFS parameters (particularly N, $\Delta\sigma^2$, and ΔE_0) of the Rh−O$_{short}$ contribution. For the remaining parameters of the models fitting the EXAFS spectra, the generally accepted error bounds (mentioned above) are larger than those determined by solely considering cross-correlation.

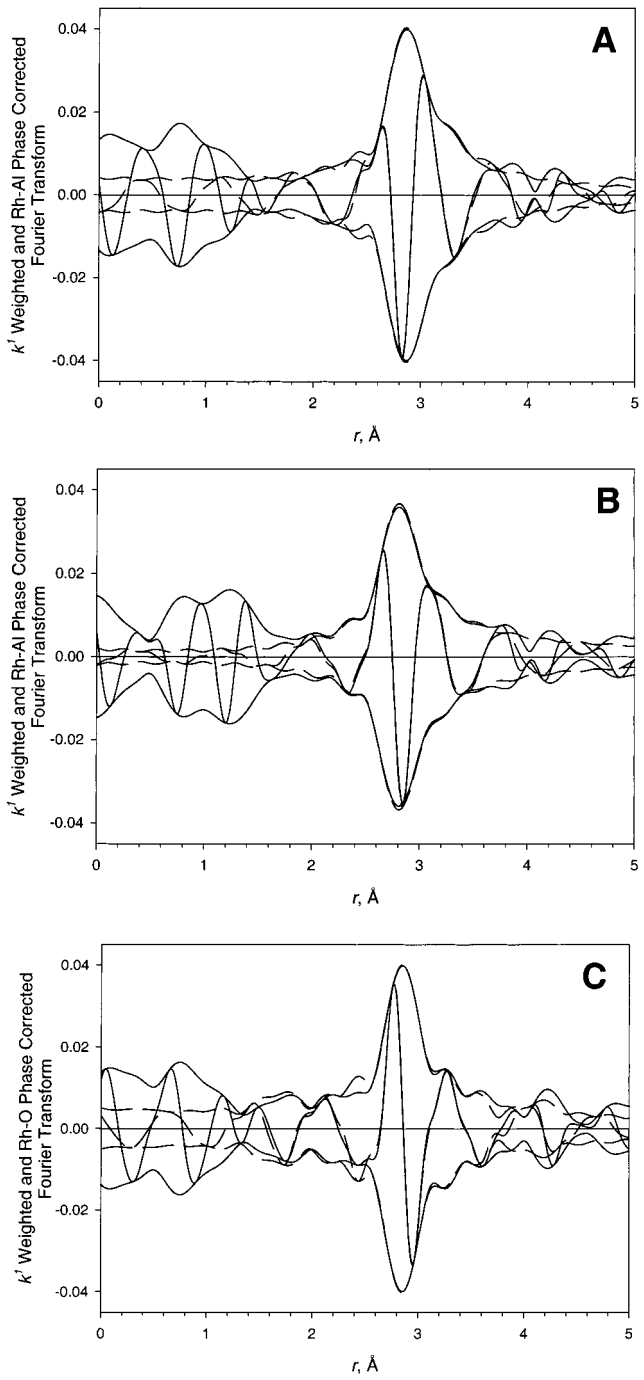

Figure 5. Proposed Rh-support contribution located at approximately 2.8 Å resulting from EXAFS data analysis for $Rh^+(CO)_2$ supported in dealuminated Y zeolite calcined at 300 °C. Displayed are the imaginary part and magnitude of the k^1-weighted Rh−X phase-corrected Fourier transform (Δk = 4.43−14.72 Å^{-1}) of the calculated Rh−X (X = Al or O_{long}) contribution according to various models (dashed lines) and the corresponding raw data with the remaining contributions (RC) subtracted from the raw data (dashed lines): (A) Model I with X = Al and RC = Rh−C, Rh−O*, Rh−O_{short}, and Rh−O; (B) Model II with X = Al and RC = Rh−C, Rh−O*, Rh−O_{short}, and Rh−O; and (C) Model III with X = O_{long} and RC = Rh−C, Rh−O*, Rh−O_{short}, and Rh−Al.

support oxygen contributions at a distance of 2.81 Å (with a coordination number of 1.7) and a contribution tentatively assigned to Rh−T (T-atom at 3.40 Å, with a coordination number of 1.0).[22] In Models I and II, these contributions are assigned to Rh−Al (at 2.75−2.73 Å with a coordination number of 1.1)[22] and tentatively to Rh−O (at 3.29−3.31 Å with a coordination number of 0.7−1.0). The values characterizing the sample calcined at 120 °C are essentially the same as these.

In summary, for each sample, the Rh−CO contributions in each model bear out the infrared spectra in showing that the supported complexes are rhodium dicarbonyls. The EXAFS parameters are in satisfactory agreement with the values for molecular analogues of rhodium dicarbonyl. The assignment of the contribution located at approximately 2.8 Å, i.e., Rh−Al for Models I and II and Rh−O for Model III (Figure 5), is the key difference between Models I and II, on the one hand, and Model III, on the other. The issue now is to discriminate among the models and specifically to determine (i) the number of oxygen atoms of the support (2 to 3) bonded to each $Rh^+(CO)_2$ complex and (ii) the bond distance, approximately 2.10 Å or approximately 2.15 Å. Because the experimental results are not sufficient to provide the discrimination, we turn to theory.

Computational Results. Because of the excess negative charge around Al sites of the zeolite framework, all cationic species in the zeolite are coordinated to oxygen centers connected to Al. In faujasites such as ours, there are thus several candidate sites where the $Rh^+(CO)_2$ complex could be coordinated: at a four-ring (T4), a six-ring (T6), or a three-hollow position next to the Al center (T5) (Figure 6). As the experiments reported here (and those reported perviously[6,23]) pertain to nearly uniform $Rh^+(CO)_2$ complexes in DAY, which is a zeolite with a low density of Al centers, we represent the zeolite for the theoretical part of the investigation as a cluster (a fragment of the zeolite) containing only one Al atom. We investigated the interaction of a single Rh^+ ion (Figure 6) as well as the interaction of the complex $Rh^+(CO)_2$ (Figure 7) with zeolite model clusters.

(a) Location of a Single Rh^+ Ion at Zeolite Clusters. The calculations show that at four-rings and at six-rings, a Rh^+ ion is bonded to the two oxygen centers of the ring connected to the Al center, as a consequence of their high basicity[24,25] (Figure 6a,c); the calculated Rh−O distances are 2.20−2.25 Å (Table 3). At the four-ring (T4 model cluster), Rh^+ is at a distance of 2.20 Å from the plane of T-atoms and interacts with two of the oxygen centers that are on the same side of the ring. At the six-ring the cation is exactly in the plane of the T-atoms since this is the only position that allows interaction with the oxygen centers of both Al−O−Si bridges in the ring (because the oxygen centers are located at different sides of the ring). At the cluster T5, Rh^+ is located in a three-hollow position (Figure 6b), close to the oxygen center of the side Al−O−Si bridge, at a Rh−O distance of 2.22 Å, and the two closest oxygen centers of the four-ring are at distances from the Rh^+ ion of 2.41 and 2.45 Å. In each of the three clusters, the O−Rh−O angles are in the range 70−76°.

The binding energy, BE, of a Rh^+ ion at each of the model clusters is about 600 kJ/mol (with respect to free Rh^+ and a negatively charged zeolite cluster). The highest BE value was

(22) The interpretation of the Rh−Al contributions characterizing each of these samples in Models I and III is tempered by their abnormally large ΔE_0 values; the corresponding value of Model II is also large. The large values of the parameter ΔE_0 arise from the dependence of EXAFS data analysis on suitable reference files. A Rh−Al alloy, with neutral metals, was employed to construct the reference file used in our analysis, whereas the Rh and Al are both charged species as in our zeolite-supported sample. The difficulty in obtaining a reference that better matches the charged nature of the Rh−Al pair in our samples results in greater than usual ΔE_0 values in the characterization of this absorber−backscatterer pair.

(23) Miessner, H. *J. Am. Chem. Soc.* **1994**, *116*, 11522.
(24) Vayssilov, G. N.; Staufer, M.; Belling, T.; Neyman, K. M.; Knözinger, H.; Rösch, N. *J. Phys. Chem. B* **1999**, *103*, 7920.
(25) Vayssilov, G. N.; Rösch, N. *J. Catal.* **1999**, *186*, 423.

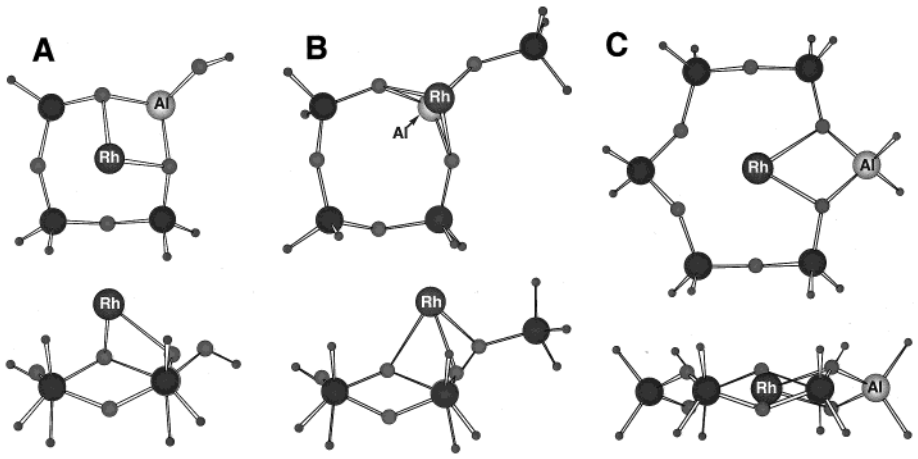

Figure 6. Location of Rh^+ ion in each cluster model used in the density functional calculations: (A) T4, four-ring; (B) T5, three-hollow site; and (C) T6, six-ring.

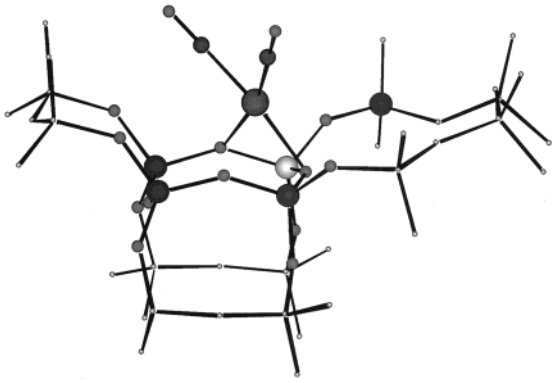

Figure 7. Location of rhodium dicarbonyl complex at a four-ring of faujasite. The atoms included in the isolated cluster model T4 are shown as circles. The dangling bonds of the cluster model are capped by hydrogen atoms.

found for the six-ring, 613 kJ/mol (Table 3). The value is greater than those representing the other clusters because of the additional interaction of the cation with the oxygen centers of Si−O−Si bridges; two of these centers are at Rh−O distances of 2.51−2.57 Å. The lowest BE was found for the T5 cluster, 577 kJ/mol, probably as a consequence of the rather short Rh−Al distance, 2.64 Å.

(b) Adsorbed Rhodium Dicarbonyl Complex. Stable structures of the $Rh^+(CO)_2$ complex were found at four-rings (the model clusters T4 and T5) but not at the six-ring.

In the optimized structure of $Rh^+(CO)_2$ at the four-ring T4 (Figure 7), each CO group is directed almost linearly in the direction of an O(z)−Rh bond (O(z) is an oxygen center of the zeolite framework), with an O−Rh−C angle of 172° and a Rh−C−O angle of 178°. The coordination at the Rh^+ center, including the two zeolite oxygen centers involved in the bonding and both CO ligands, is essentially planar. The O−Rh−O angle is 76°, and the C−Rh−C angle is 90.4°. The coordination of CO results in shorter O(z)−Rh bonds, by 0.02−0.05 Å relative to those of the cluster with a bare Rh^+, and the cation is shifted 0.40 Å farther from the plane of the ring. The Rh−C bond length in adsorbed $Rh^+(CO)_2$ is almost the same as that calculated for gas-phase $Rh^+(CO)_2$; however, the C−O bonds after adsorption are slightly longer, by 0.01 Å. This result suggests stronger π-back-donation from the cation to the antibonding π^*-orbitals of CO in the adsorbed complex than in the free complex.

The whole complex $Rh^+(CO)_2$ in the four-ring, BE = 654 kJ/mol, is more stable (by 65 kJ/mol) than the bare Rh^+ in the four-ring, BE = 589 kJ/mol (Tables 4 and 5). Similarly, the BE of CO on Rh^+ at the four-ring T4, 211 kJ/mol per CO molecule, is greater by 32 kJ/mol than that of CO on a free Rh^+, 179 kJ/mol. Thus, we infer that the bond lengths and BE values show a synergy between the interaction of Rh^+ with the zeolite support and with two CO molecules; each interaction strengthens the other.

Table 4. Calculated Distances (Å) and Binding Energies (kJ/mol) of Free and Adsorbed Complex $Rh^+(CO)_2$

	$Rh^+(CO)_2$	$Rh^+(CO)_2$-T4	$Rh^+(CO)_2$-T5
distances			
C−O[a]	1.146	1.156, 1.157	1.156, 1.156
Rh−C	1.878	1.877, 1.881	1.881, 1.885
Rh−O(Al)		2.19, 2.20	2.18, 2.19
Rh−O(Si)		3.33, 3.85	3.17, 3.72
Rh−O(OH)		3.24	3.51
Rh−Al		2.80	2.84
Rh−Si		3.36, 3.39, 3.86	3.28, 3.31, 3.70
binding energies			
$Rh^+(CO)_2$ *b*		654	633
2 CO	358[c]	422[d]	414[d]
per CO	179	211	207

[a] The calculated C−O distance in the free CO molecule is 1.145 Å. [b] Binding energy (BE) of the complex calculated as $E[Rh^+(CO)_2-Tn] - E[Rh^+(CO)_2] - E[Tn^-]$ (where Tn is T4 or T5). [c] BE of two ligand molecules calculated as $E[Rh^+(CO)_2] - 2E[CO] - E[Rh^+]$. [d] BE of two ligand molecules calculated as $E[Rh^+(CO)_2-Tn] - 2E[CO] - E[Rh-Tn]$.

The geometry optimization of the complex $Rh^+(CO)_2$ at the model cluster T5 was started with a structure representing adsorption of the Rh^+ ion at the three-hollow site of this cluster (Figure 6b). During the optimization, however, the $Rh^+(CO)_2$ complex was found to shift in the direction of the four-ring of the T5 cluster, and the final structure is very similar to that of $Rh^+(CO)_2$ adsorbed at the T4 cluster (Table 4). A small difference between the two is that the central cation is shifted farther to the center of the four-ring in the T5 model. The distances from the Rh center to the Al center and the oxygen center of the side $OSiH_3$ group are longer for the $Rh^+(CO)_2$ complex at the model cluster T5 than for this complex at the model cluster T4, whereas the distances between the Rh center and the oxygen centers of Si−O−Si bridges of the ring are shorter. The Rh−C distances in the two models differ by less than 0.01 Å, and the C−O bond lengths are the same. The calculated BE of $Rh^+(CO)_2$ adsorbed at the T5 cluster is lower by 20 kJ/mol than that at the T4 cluster (Table 4). Furthermore, the BE of a CO ligand bonded to Rh^+ at the T5 cluster is slightly

Table 5. Frequencies (cm^{-1}) and Intensities (in parentheses, km/mol) of Other Vibrational Modes of the Complex $Rh^+(CO)_2$−T4 with Two ^{12}CO or Two ^{13}CO Ligand Molecules

C isotope in sample		C−Rh		Rh−C−O in-plane and out-of-plane bending modes				Rh-zeolite	
^{12}CO	calcd	483 (12)	471 (7)	597(14)	494(3)	442(2)	419(0.3)	358(34)	341(28)
	exptl	500[a]	440[a]						
^{13}CO	exptl	492[b]	464[b]						
	calcd	474 (9)	461 (5)	581(11)	481(6)	430(2)	408(0.3)	358(34)	341(28)
	exptl	490[a]	430[a]						

[a] Estimated from combination bands of rhodium dicarbonyl in DAY.[6] [b] Frequencies of complex *cis*-$[RhCl_2(CO)_2]^-$.[27]

reduced (relative to binding to Rh^+ at the T4 cluster), to 207 kJ/mol.

In summary, these results of the geometry optimizations of $Rh^+(CO)_2$ at the two zeolite cluster models indicate that the cation prefers a (pseudo-square)-planar four-coordinated geometry, as in typical inorganic or organometallic complexes of Rh^+.

In contrast, the calculations show that as a result of coordination of two CO molecules to a Rh^+ ion at the six-ring T6, the $Rh^+(CO)_2$ moves farther from the plane of the ring formed by the T-atoms. Thus, Rh^+ remains bound to only one of the framework oxygen centers connected to an Al atom, since the second oxygen center remains on the other side of the ring. Consequently, a planar Rh^+ complex with four ligands cannot be formed. This situation is different from that involving zeolite six-rings with two or three Al centers (as occurs for zeolites with higher Al:Si ratios), whereby two or three oxygen centers connected to Al atoms are directed to one side of the six-ring[24] and a stable pseudo-square-planar configuration of an adsorbed complex can be achieved also at six-rings.

(c) Vibrational Frequencies. The calculated vibrational frequencies of the C−O stretching mode of $Rh^+(CO)_2$ adsorbed at the model four-ring T4 (Table 1) differ by only 1−11 cm^{-1} from the experimental infrared frequencies. The close agreement between calculated and experimental values of the two low-frequency satellite peaks, generated by mixed-isotope dicarbonyl complexes $Rh^+(^{12}CO)(^{13}CO)$ present in the sample corresponding to the natural ^{13}C abundance, verifies the structural model. We also compared the calculated and experimental frequencies for the various combinations of $^{12}C/^{13}C$ and $^{16}O/^{18}O$ isotope-labeled CO molecules reported in ref 6. In all six cases, the calculated frequencies differ at most by 7 cm^{-1} from the experimental values, and the comparison supports the proposition that the model structure $Rh^+(CO)_2$−T4 is a good representation of $Rh^+(CO)_2$ in DAY (as shown in Figure 7).

The calculated intensity ratio of symmetric and antisymmetric modes I_{sym}/I_{asym}, 0.72, is somewhat larger than the value of 0.57 back-calculated from the C−Rh−C angle reported by Miessner et al.,[6,23] but it corresponds to the present infrared measurements, 0.67 and 0.75.[26]

We also calculated the frequencies and intensities of other modes of the adsorbed complex (Table 5). All these vibrations have low intensities (0.3−34 km/mol) relative to the C−O stretching mode (400−600 km/mol) and low frequencies, <600 cm^{-1}. Because of the strong absorbance of the zeolite itself in this spectral region, these bands could hardly be detected directly, but combination modes with the C−O stretching vibration were observed in the infrared spectra. Such combination bands have been reported for $Rh^+(CO)_2$ in DAY.[6] On the basis of their similarity to the bands of the well-characterized anion *cis*-$[RhCl_2(CO)_2]^-$, Miessner et al.[6] assigned these bands to combinations of the symmetric and antisymmetric ν_{CO} and ν_{RhC} modes (Table 5). Taking into account the substantial experimental uncertainties in the frequencies ν_{RhC} of $Rh^+(CO)_2$ in DAY, we infer that the calculated values are in satisfactory agreement with experiment, with a typical difference of about 30 cm^{-1}. The differences between the calculated frequencies ν_{RhC} and the experimental results characterizing *cis*-$[RhCl_2(CO)_2]^-$ are smaller, less than 10 cm^{-1}.[27]

Bonding Position of $Rh^+(CO)_2$ in DAY Zeolite. The ν_{CO} peaks of the infrared spectrum of each sample characterize the species as a rhodium *gem*-dicarbonyl with Rh in the +1 oxidation state.[28,29] Thus, candidate bonding sites in the zeolite are cation exchange sites associated with framework Al.[30,31] During dealumination to prepare DAY from zeolite Y, most of the framework Al is removed, so that only well-separated Al centers remain. Thus, there are only a few candidate bonding sites for $Rh^+(CO)_2$.

The infrared spectra are consistent with the hypothesis that $Rh^+(CO)_2$ is bonded near framework Al centers. Miessner et al.[6] did not observe acidic hydroxyl site peaks after the formation of supported $Rh^+(CO)_2$ from supported rhodium crystallites was complete. In our infrared spectra, no acidic hydroxyl peaks were found.[14] Since the acidic hydroxyl peaks disappear after $Rh^+(CO)_2$ is bonded to the surface (or is formed on it), we infer that the bonding site of $Rh^+(CO)_2$ is associated with the acidic hydroxyl sites, which are associated with framework Al centers.

Further indications that $Rh^+(CO)_2$ bonds near framework Al centers are provided by the effect of the zeolite Si:Al ratio on the infrared spectra. The peaks representing $Rh^+(CO)_2$ bonded to zeolite NaY[5] that had been calcined at 300 °C and had a low Si:Al ratio (approximately 2.6) are considerably broader than those observed for the complex bonded to DAY (Si:Al approximately 100) which had been calcined at 300 °C (Figure 1).[32]

The ν_{CO} peaks in the spectrum of $Rh^+(CO)_2$ bonded to zeolite NaY[5] calcined at 300 °C are shifted to lower frequencies, by 34 and 36 cm^{-1}, relative to those of the same complex bound to DAY calcined at 300 °C. This observation is consistent with Miessner's[6] observation of how the Si:Al ratio influences the position of ν_{CO} peaks in the infrared spectra of their zeolite Y-supported $Rh^+(CO)_2$. Since the ν_{CO} peak position is primarily

(26) When we used the calculated ratio I_{sym}/I_{asym} to deduce the C−Rh−C angle, we obtained a value of 99°, although the angle employed in calculating the frequencies and intensities is 90.4°, as determined in the geometry optimization. This comparison shows that the estimate of the angle between two ligand molecules on the basis of the intensity ratio of the symmetric and antisymmetric vibrations is not accurate.

(27) Browning, J.; Goggin, P. L.; Goodfellow, R. J.; Norton, M. G.; Rattray, A. J. M.; Taylor, B. F.; Mink, J. *J. Chem. Soc., Dalton Trans.* **1977**, 2061.

(28) Yates, J. T., Jr.; Duncan, T. M.; Worley, S. D.; Vaughn, R. W. *J. Chem. Phys.* **1979**, *70*, 1219.

(29) Solymosi, F.; Knözinger, H. *J. Chem. Soc., Faraday Trans.* **1990**, *86*, 389.

(30) Sauer, J.; Ugliengo, P.; Garrone, E.; Saunders: V. R. *Chem. Rev.* **1994**, *94*, 2095.

(31) van Santen, R. A.; Kramer, G. J. *Chem. Rev.* **1995**, *95*, 637.

(32) The broadening of the peaks representing $Rh^+(CO)_2$ bonded to zeolite NaY[5] was so pronounced that the natural-abundance ^{13}CO peaks were not found in the spectrum although they are evident in the spectra of the present samples.

influenced by the local structure,[33] we infer from the effect of the Si:Al ratio that $Rh^+(CO)_2$ is situated near a framework Al center. This result of the infrared spectroscopy is important in narrowing the possible candidate structures of the supported rhodium dicarbonyl.

Analysis of the EXAFS data led to three plausible structural models, and the data are not sufficient to determine the number of O(z) centers coordinated at short (approximately 2.1 Å) and long (approximately 2.8 Å) distances from Rh. The short Rh−O distances (2.09−2.16 Å) determined by fitting the data in accord with each of the three models are bonding distances that compare well with previous EXAFS observations for $Rh^+(CO)_2$ supported on metal oxides.[7,8] Short Rh−O distances were reported for $Rh^+(CO)_2$ on γ-Al_2O_3, namely, 2.12 Å with a coordination number of 3, by van't Blik et al.,[8] and 2.04 Å with a coordination number of 7, by Binsted et al.[7] The coordination numbers found in our work for the $Rh-O_{short}$ contribution (namely, 3, 2, and 2 for Models I, II, and III, respectively) are in line with the observations of van't Blik, but not with those of Binsted et al. The latter result is difficult to understand because it implies a 26-electron complex. A similarly short $Rh-O_{short}$ bond distance (2.05 Å) as found here was also determined by Weber et al.[5] for $Rh^+(CO)_2$ supported on zeolite NaY. Thus, the short Rh−O distances observed in our investigation are consistent with previous results characterizing oxide-supported complexes, and these literature data do not help to discriminate among our candidate models.

The $Rh-O_{long}$ contribution used in the Model III representation of the EXAFS data essentially matches what has been reported for highly dispersed oxide- and zeolite-supported noble metals. However, a lack of consistency in the observation of $Rh-O_{long}$ contributions for highly dispersed oxide-supported transition metals, even for a single support, e.g., zeolite NaY, makes it difficult to use the literature reports of $Rh-O_{long}$ contributions in EXAFS spectra as a basis for preferring Model III.[34]

Thus, we turn to our density functional model cluster calculations as a basis for discriminating among the candidate structural models. The following comparison of the calculated and EXAFS results is based on the optimized structures of the $Rh^+(CO)_2$ complexes adsorbed at the model clusters T4 and T5.

The EXAFS values for the Rh−C and Rh−O* distances are 1.84−1.86 and 2.96−3.05 Å for the samples supported in DAY calcined at 120 and 300 °C, respectively. In each case, the calculated distances, 1.88 and 3.03−3.04 Å, respectively, match the corresponding EXAFS data well (Table 2).

However, further analysis is needed to clarify the location of the Rh cation in the zeolite. According to the EXAFS data, there are three Rh−X contributions (where X denotes zeolite framework centers: O, Al, or Si), at distances of 2.09−2.16, 2.70−2.80, and 3.20−3.40 Å. The contributions of different zeolite centers to these groups, as expected on the basis of the theoretical results (Table 4), are shown in Table 2. Two oxygen centers are at a shorter distance, $Rh-O_{short}$, at about 2.20 Å, one Al center is at a distance of about 2.80 Å, and a third contribution would be a superposition of one O center at longer distance, Rh−O, and two Si centers.

In Table 2 we compare the calculated values with the EXAFS data characterizing the two samples, refined according to Models I, II, and III. The Rh−Al and the longer Rh−O distances found for Models I and II as well as the Rh−T distance found for Model III fit the calculated values for each sample. The differences between the two sets of data are not substantial if one takes into account that these centers at distances of 2.70−2.80 and 3.20−3.40 Å from the Rh center represent the second and third coordination spheres and that there is some averaging among different Rh−X distances.

The largest difference between calculated and EXAFS values is associated with the bond between the Rh cation and the closer zeolite oxygen centers. This is a nearest-neighbor bonding distance, and one expects it to be reproduced with higher accuracy than the distances between Rh^+ and the other zeolite centers referred to above. The calculations suggest two oxygen centers at 2.18−2.20 Å from the Rh^+, whereas the EXAFS refinement leading to Models I and III corresponds to 2.2−3.5 oxygen centers bonded to rhodium dicarbonyl supported on DAY calcined at either 120 or 300 °C, with $Rh-O_{short}$ distances of 2.09−2.12 Å. The cluster calculations show that the adsorption of $Rh^+(CO)_2$ at the three-hollow position of the zeolite (modeled by the cluster T5) is unlikely; thus, the coordination number *N* should be close to 2. Consequently, serious doubt is cast on Models I and III because their $Rh-O_{short}$ distances are approximately 0.1 Å shorter than those of the cluster calculations. Skepticism regarding these models is increased because Model I has essentially one too many oxygen atoms coordinated at a short distance to the Rh^+ ion and Model III, although having the right number of oxygen atoms coordinated to Rh^+ at a short distance has a $Rh-O_{long}$ contribution for which the cluster calculations indicate a Rh−Al contribution.

In contrast, satisfactory agreement between the experimental and theoretical $Rh-O_{short}$ bond distances was obtained for Model II, according to which the $Rh-O_{short}$ contributions are represented by coordination numbers of 1.8 and 1.9 and bond distances of 2.16 and 2.15 Å for the zeolites calcined at 120 and 300 °C, respectively. Within the typical experimental uncertainty, the measured coordination numbers (1.8 and 1.9) are the same as that of each of the cluster models (2). Bond lengths calculated at the Becke−Perdew level of DFT are usually slightly longer than experimental values,[35,36] by about 0.02−0.04 Å for bonds between a transition metal center and light main-group atoms. Typical experimental uncertainties in EXAFS bond distances are ±0.02 Å. Thus, the difference between the observed and calculated $Rh-O_{short}$ distances for Model II (0.03−0.05 Å) is consistent with the expected uncertainties. Consequently, the EXAFS-derived Model II and the DFT cluster calculations are concluded to be in good agreement with each other, whereas Models I and III, which do not agree well with the calculations, are rejected.

The close agreement of calculated and experimental vibrational frequencies (Table 1) provides further support for the hypothesis that $Rh^+(CO)_2$ in DAY is bound to two oxygen centers of a four-ring with a structure similar to that of model cluster T4 (Figure 7) and the EXAFS-derived Model II. Thus, the infrared data bolster the selection of the structural model.

(33) We recognize that the vibrational frequency of adsorbed CO is affected by long-range fields, such as the Madelung field. However, the assertion that the local effects dominate the position of the ν_{CO} bands is supported by the close agreement (Table 1) between the experimental frequencies and those calculated using only a localized fragment of the zeolite structure to represent the support.

(34) The distance $Rh-O_{long}$ has been shown to vary significantly as a function of sample reduction for TiO_2 (2.60−2.78 Å), but not for γ-Al_2O_3 (2.73−2.76 Å) supports.[62] No $Rh-O_{long}$ contributions were found for Rh_6 in zeolite NaY,[46,63] but for zeolite NaY supported $Rh^+(CO)_2$ such a contribution was observed at about 2.5 Å.[5]

(35) Görling, A.; Trickey, S. B.; Gisdakis, P.; Rösch, N. In *Topics in Organometallic Chemistry*; Brown, J., Hofmann, P., Eds.; Springer: Heidelberg, 1999; Vol. 4, p 109.

(36) Goellner, J. F.; Neyman, K. M.; Mayer, M.; Nörtemann, F.; Gates, B. C.; Rösch, N. *Langmuir* **2000**, *16*, 2736.

Discussion

Support Surfaces as Multidentate Ligands. The concept of the support as a multidentate ligand,[37] which has been reinforced experimentally[38] and theoretically[9] for rhenium subcarbonyls on MgO, has been applied by several groups for rhodium carbonyls on oxide supports. Basset and Choplin[39] used simple electron counting when assessing the support as a multidentate ligand, assigning 0, 1, and 2 electrons to Al^{3+}, O−M, and O surface ligands, respectively. Basset and Choplin[39] proposed that $Rh^+(CO)_2/\gamma$-Al_2O_3 incorporates two support oxygen ligands, corresponding to a 16-electron complex. van't Blik et al.[8] represented $Rh^+(CO)_2/\gamma$-Al_2O_3 as an 18-electron complex with oxygen as a two-electron donor and reported the following EXAFS parameters for $Rh-O_{short}$: $N = 3$ and $R = 2.12$ Å. Thus, these two models differ only in the assumed number of oxygen ligands of the support. In contrast, the model of Binsted et al.[7] ($Rh-O_{short}$: $N = 7$, $R = 2.04$ Å) corresponds to a hypervalent 26-electron complex and is regarded as unlikely.

In accordance with van't Blik et al.,[8] the 18-electron systems indicated by Models I and III increase the electron count of the $Rh^+(CO)_2$ complex by 2 when it is coordinated to the surface. Our results for $Rh^+(CO)_2$ in DAY according to Model II are similar to the model of Basset and Choplin[39] represented as a 16-electron complex which maintained a pseudo-square-planar geometry upon adsorption of the rhodium dicarbonyl.[40] We are convinced that theoretical results such as those presented here add a strong component to the structural model and that electron counting alone is not always sufficient for discrimination among models based on spectroscopic results.

Strengths and Limitations of Methods for Characterizing Highly Dispersed Metals and Metal Complexes Supported by Zeolites and Metal Oxides. In a family of supported metal structures ranging from particles to clusters and ultimately to mononuclear metal complexes, the metal−support interface becomes increasingly important as the size of the metal species decreases. Correspondingly, the number of applicable characterization techniques becomes smaller. EXAFS spectroscopy is one of the few techniques capable of characterizing supported metal particles smaller than the coherence limit and at concentrations below the detection limit of X-ray diffraction. Thus, EXAFS spectroscopy is of major importance for such samples. However, its limitations can lead to ambiguous results, as exemplified by the present work. We discuss some of these limitations below and stress the importance of theory as a complement to this experimental method.

With good EXAFS data it is straightforward to detect and identify metal−metal contributions. By showing that there were no detectable Rh−Rh contributions in our samples, EXAFS spectroscopy was effective in demonstrating that the $Rh^+(CO)_2$ species were largely isolated from each other in the zeolite. However, the limits of EXAFS spectroscopy become evident in the characterization of the metal−support interface. Metal-edge EXAFS spectroscopy is not able to determine unambiguously the coordination numbers of metal−low-Z backscatterers, as shown by the conflicting values of $Rh-O_{short}$ coordination numbers reported for $Rh^+(CO)_2$ on γ-Al_2O_3[7,8] and by the differences in the several models reported here for this complex in DAY, all of which agree almost equally well with the data. The appropriate conclusion based on EXAFS spectroscopy alone is that the $Rh-O_{short}$ coordination number for each sample is approximately 2 or 3; the uncertainty in the bond distances is about 0.1 Å.

Furthermore, the available experimental methods were not sufficient to identify the backscatterer near Rh at a distance of approximately 2.8 Å. This contribution in the EXAFS spectra appears as an asymmetric peak for each sample when analyzed according to Models I and II, which is indicative of multicontribution interference. Hence, $Rh-O_{long}$ and Rh−Al contributions cannot be separated or differentiated on the basis of the EXAFS data. It is also possible that the asymmetry arises from interference associated with other contributions, such as Rh−O*. Furthermore, the EXAFS technique is limited by the number of statistically justifiable parameters that can be used in a model fit of the spectrum and by the amount of information that can be carried between *k* space and *r* space by a finite and discrete Fourier transformation. These limitations are related to each other; the latter dictates the former. These issues determine whether adding a spectral component (shell) improves the fit because it truly represents the structure or rather because terms are added to the Fourier series used to represent the spectrum. We emphasize that the quality of our EXAFS data is high; the limitations illustrated here with our data and analysis are applicable to the EXAFS technique with some generality.

In summary, EXAFS spectroscopy is valuable for characterizing structures that are dispersed in low concentrations in solids, being most valuable when the structures are site isolated and nearly uniform. However, the technique is limited, particularly in its ability to determine the structures of sample in which two or more backscatterers of similar potential (phase) are located at nearly the same distance from the absorbing atom. Calculations based on density functional theory are a valuable complement to EXAFS spectroscopy, helping to resolve the ambiguities in the data.

Experimental and Theoretical Methods

Materials and Sample Preparation. Sample syntheses and transfers were performed in the absence of moisture and air with a Braun MB-150M drybox (purged with N_2 recirculating through traps for O_2 and moisture) and a double manifold Schlenk vacuum line. N_2 (99.999%) flowed through traps containing particles of Cu and of zeolite 4A to remove traces of O_2 and water, respectively. *n*-Hexane was dried over sodium benzophenone ketyl and deoxygenated with flowing N_2 prior to use. [$Rh(CO)_2$(acac)] (Strem, 99%) was used as received.

Dealuminated zeolite HY, with a Si:Al ratio of approximately 100, was obtained from Degussa. Calcination was carried out by flowing O_2 through a bed of the zeolite while ramping the temperature to 120 °C, holding the temperature at 120 °C for 3 h, and then ramping the temperature to the value referred to as the calcination temperature and holding for 3 h. The O_2 treatment was immediately followed by evacuation of the sample for 14 h at the calcination temperature. The zeolite was then cooled to room temperature under vacuum, isolated, and stored in a N_2-filled glovebox until use. Two calcination temperatures were used, 120 and 300 °C.

In the glovebox, [$Rh(CO)_2$(acac)] was combined with the calcined zeolite in a Schlenk flask with the mixture containing 1 wt % Rh, so that the final zeolite samples had Rh:Al atomic ratios of approximately 1:2. Dried and deoxygenated *n*-hexane was then introduced by cannula into each sample in a Schlenk flask. The resultant slurry was stirred for 1 day, and the solvent was removed by evacuation (pressure $<10^{-3}$ Torr) for 1 day. The resultant samples were stored in a drybox.

Characterization by Infrared Spectroscopy. A Bruker IFS 66v spectrometer with a spectral resolution of 4 cm^{-1} was used to collect infrared spectra of the sample powders. To prepare an optically thin sample allowing detection of minor peaks, a small amount of powder was pressed between two windows in an environmentally controlled infrared cell. Each reported spectrum is the average of 64 scans.

(37) Deutsch, S. E.; Chang, J.-R.; Gates, B. C. *Langmuir* **1993**, *9*, 1284.
(38) Papile, C. J.; Gates, B. C. *Langmuir* **1992**, *8*, 74.
(39) Basset, J.-M.; Choplin, A. *J. Mol. Catal.* **1983**, *21*, 95.
(40) The organometallic precursor used in the sample synthesis, Rh(CO)$_2$(acac), is a square-planar 16-electron complex.

Characterization by X-ray Absorption Spectroscopy. EXAFS spectra were collected at beam line 4-1 of the Stanford Synchrotron Radiation Laboratory (SSRL) at the Stanford Linear Accelerator Center, Stanford, CA. The ring current was 50−100 mA, and the storage ring operated with an electron energy of 3 GeV.

In a N_2-filled drybox at the synchrotron, powder samples were pressed into self-supporting wafers. The mass of each wafer was chosen to give an X-ray absorbance of approximately 2.5 at the Rh K edge. After being pressed into a wafer, the sample was loaded into an EXAFS cell,[41] sealed under a positive N_2 pressure, and removed from the drybox. The cell was then evacuated (10^{-5} Torr), and the sample was aligned in the X-ray beam and cooled to nearly liquid nitrogen temperature. EXAFS spectra were then collected in transmission mode. The Si (220) double crystal monochromator was detuned by 20% at the Rh K edge to suppress higher harmonics in the X-ray beam.

Computational Methods and Structural Models. (a) Density Functional Theory. The calculations were carried out with the density functional program ParaGauss[42] using the gradient-corrected exchange-correlation functional suggested by Becke (exchange) and Perdew (correlation).[43] Gaussian-type basis sets, contracted in generalized form, were employed to describe the Kohn−Sham orbitals: (6s1p) → [3s1p] for H, (9s5p1d) → [5s4p1d] for O and C, (12s9p1d) → [6s4p1d] for Al and Si, and (19s15p10d) → [8s6p4d] for Rh.[44] The structures of the clusters were optimized using analytical energy gradients.[45]

The initial structures of the zeolite four-ring (T4) and six-ring (T6) model clusters are taken from previous work.[24,25] Only clusters containing one aluminum center were considered. The free valences of the T-atoms were saturated by H atoms. In the four-ring T4, one of the saturating H atoms at the Al center was substituted by an OH group (Figure 6a). To model the location of the guest complex at a three-hollow position, we also considered an additional model cluster, T5. It originates from the four-ring; however, the OH group at the Al center is replaced by an $OSiH_3$ (Figure 6b). This cluster contains five T-atoms, hence its designation T5. The position of the rhodium cation and the geometry of the guest complexes were optimized with the positions of the T-atoms of the model zeolite rings and the H atoms saturating them kept fixed. These restrictions during the geometry optimization reflect the observation[6,23] that inclusion of the guest complex does not induce any noticeable change in the structure of the zeolite material. In the structure optimization of the model cluster T5, the structure of the $OSiH_3$ fragment was allowed to relax.

After optimization of a complete cluster model, a constrained frequency analysis was carried out whereby the vibrational modes of the CO ligands and rhodium with respect to the zeolite fragment were taken into account. Normal harmonic vibrational frequencies were calculated by diagonalizing the mass weighted force constant matrix in internal coordinates. The force constants were obtained numerically by finite differences of analytical energy gradients. The calculated harmonic vibrational frequencies of the C−O stretching modes were corrected with +32 cm^{-1}, which is the difference between the calculated (2111 cm^{-1}) and the experimental frequency of a free ^{12}CO molecule (2143 cm^{-1}). The same correction was also applied to ^{13}CO; the calculated and experimental frequencies are 2064 and 2096 cm^{-1}, respectively.

(b) Analysis of EXAFS Data. Analysis of the EXAFS data was carried out with a difference file technique[46−48] using the software XDAP.[49] No attempt was made to account for the small atomic X-ray absorption fine structure (AXAFS)[50,51] (the low-r portion) of the spectrum other than by application of standard background removal techniques[52] (r is the distance from the absorbing atom, Rh). Iterative fitting was carried out until excellent agreement was attained between the calculated k^0-, k^1-, k^2-, and k^3-weighted data and the postulated model;[46−48] otherwise, the model was rejected.

Experimentally determined reference files prepared from EXAFS data representing materials of known structure were used in the analysis. EXAFS data characterizing a rhodium foil and Rh_2O_3 were used for the phase shifts and backscattering amplitudes of the Rh−Rh and Rh−$O_{support}$ interactions. [$Ru_3(CO)_{12}$], with only terminal CO ligands, mixed with BN, was used to obtain the phase shifts and backscattering amplitudes used in analyzing the Rh−C and Rh−O* interactions (O* is carbonyl oxygen). The transferability of the phase shifts and backscattering amplitudes for neighboring atoms in the periodic table has been justified experimentally.[53] It was necessary to use a reference that exhibited multiple scattering, such as [$Ru_3(CO)_{12}$], because the near linearity of the Rh−C−O moieties makes the influence of multiple scattering in the Rh−O* shells significant. The Rh−Al reference file was calculated by using the code FEFF 7.0[54] and structural parameters representing a Rh−Al alloy.[55] Details of the preparation of the reference files are presented elsewhere.[56−58] A summary of the parameters[55,59−61] used to construct the reference files from the EXAFS data is given in the Supporting Information.

Conclusions

Infrared and EXAFS spectroscopies and calculations based on density functional theory were used to determine the structure and location of rhodium dicarbonyls in highly dealuminated zeolite Y. Infrared spectra identify the surface species as $Rh^+(CO)_2$; the sharp CO bands suggest unique species. EXAFS spectra identify the species as site isolated rhodium dicarbonyls and provide estimates of the number of support oxygen centers interacting with each Rh center and the corresponding Rh−$O_{support}$ distance. Models consistent with these data were constructed and their structures optimized, with the results indicating that $Rh^+(CO)_2$ is bonded at two of the oxygen centers in a four-ring containing one Al center. The theoretical results were used to discriminate among candidate structural models based on the experimental results; they indicated a (pseudo-square)-planar complex with two CO ligands bonded cis to rhodium. The calculated distances and vibrational frequencies

(41) Jentoft, R. E.; Deutsch, S. E.; Gates, B. C. *Rev. Sci. Instrum.* **1996**, *67*, 2111.
(42) ParaGauss 2.0, Belling, T.; Grauschopf, T.; Krüger, S.; Nörtemann, F.; Staufer, M.; Mayer, M.; Nasluzov, V. A.; Birkenheuer, U.; Rösch, N.; Technische Universität München: München, 1999.
(43) (a) Becke, A. D. *Phys. Rev. A* **1988**, *38*, 3098. (b) Perdew, J. P. *Phys. Rev. B* **1986**, *33*, 8822. Perdew, J. P. *Phys. Rev. B* **1986**, *34*, 7406.
(44) (a) Ferrari, A. M.; Neyman, K. M.; Rösch, N. *J. Phys. Chem. B* **1997**, *101*, 9292. (b) Godbout, N.; Salahub, D. R.; Andzelm, J.; Wimmer, E. *Can. J. Chem.* **1992**, *70*, 560.
(45) Nasluzov, V. A.; Rösch, N. *Chem. Phys.* **1996**, *210*, 413.
(46) Weber, W. A.; Gates, B. C. *J. Phys. Chem. B* **1997**, *101*, 10423.
(47) van Zon, J. B. A. D.; Koningsberger, D. C.; van't Blik, H. F. J.; Sayers, D. E. *J. Chem. Phys.* **1985**, *82*, 5742.
(48) Kirlin, P. S.; van Zon, F. B. M.; Koningsberger, D. C.; Gates, B. C. *J. Phys. Chem.* **1990**, *94*, 8439.
(49) Vaarkamp, M.; Linders, J. C.; Koningsberger, D. C. *Physica B* **1995**, *209*, 159.
(50) Ramaker, D. E.; Mojet, B. L.; Koningsberger, D. C.; O'Grady, W. E. *J. Phys. Condens. Matter* **1988**, *10*, 8753.
(51) Ramaker, D. E.; Quan, X.; O'Grady, W. E. *Chem. Phys. Lett.* **1999**, *299*, 221.
(52) Cook, J. W., Jr.; Sayers, D. E. *J. Appl. Phys.* **1981**, *52*, 5024.
(53) Duivenvoorden, F. B. M.; Koningsberger, D. C.; Uh, Y. S.; Gates, B. C. *J. Am. Chem. Soc.* **1986**, *108*, 6254.
(54) (a) Zabinsky, S. I.; Rehr, J. J.; Ankudinov, A.; Albers, R. C.; Eller, M. J. *Phys. Rev. B.* **1995**, *52*, 2995. (b) Ankudinov, A. Ph.D. Dissertation, University of Washington, 1996.
(55) Donnay, J. D. H.; Ondik, H. M. *Crystal Data Determinative Tables*, 3rd ed.; U.S. Department of Commerce, National Bureau of Standards and the Joint Committee on Powder Diffraction Standards: Washington, DC, 1973; Vol. II, p C-4.
(56) van Zon, F. B. M.; Maloney, S. D.; Gates, B. C.; Koningsberger, D. C. *J. Am. Chem. Soc.* **1993**, *115*, 10317.
(57) van Zon, J. B. A. D. Dissertation, Eindhoven University of Technology, The Netherlands, 1988.
(58) van Zon, J. B. A. D.; Koningsberger, D. C.; Gates, B. C. *J. Chem. Phys.* **1985**, *82*, 5742.
(59) Wycoff, R. W. G., Ed. *Crystal Structures*, 2nd ed.; Wiley: New York, 1963; Vol. 1, p 10.
(60) Coey, J. M. D. *Acta Crystallogr.* **1970**, *B26*, 1876.
(61) Mason, R.; Rae, A. I. M. *J. Chem. Soc. A* **1968**, 778.
(62) Martens, J. H. A.; Prins, R.; Zandberge, H.; Koningsberger, D. C. *J. Phys. Chem.* **1988**, *92*, 1903.
(63) Rao, L.-F.; Fukuoka, A.; Kosugi, N.; Kuroda, H.; Ichikawa, M. *J. Phys. Chem.* **1990**, *94*, 5317.

agree well with the infrared and EXAFS data. The results demonstrate the inadequacy of the experimental methods alone in elucidating the structure of a relatively simple and uniform surface metal complex and the value of theory in discriminating among the structural models postulated on the basis of the experimental results.

Acknowledgment. We thank H. Miessner for helpful discussions, W. A. Weber for infrared data, and the staff of the Stanford Synchrotron Radiation Laboratory for their assistance. B.C.G. and J.F.G. acknowledge support from the U.S. Department of Energy, Office of Energy Research, Office of Basic Energy Sciences, Division of Chemical Sciences. G.N.V. is grateful to the Alexander von Humboldt foundation for a fellowship. The work of N.R. is supported by the Deutsche Forschungsgemeinschaft and the Fonds der Chemischen Industrie. The EXAFS data were analyzed with XDAP.[49] The EXAFS experiments were done at the Stanford Synchrotron Radiation Laboratory, which is operated by Stanford University for the Department of Energy, Office of Basic Energy Sciences.

Supporting Information Available: Tables of fit diagnostic parameters and crystallographic data and figures showing infrared spectra in the OH stretching region of $Rh^{+}(CO)_2$ and standard deviations in the EXAFS χ function (PDF). This material is available free of charge via the Internet at http://pubs.acs.org.

JA001209F